International Journal of Nanomedicine

Dovepress
open access to scientific and medical research

Open Access Full Text Article

ORIGINAL RESEARCH

Hsa_circ_0000069 Knockdown Inhibits Tumorigenesis and Exosomes with Downregulated hsa_circ_0000069 Suppress Malignant Transformation via Inhibition of STIL in Pancreatic Cancer

This article was published in the following Dove Press journal:
International Journal of Nanomedicine

Zhenyu Ye*
Zhaobi Zhu*
Jiaming Xie
Zhenyu Feng
Yecheng Li
Xiangrong Xu
Wei Li
Wei Chen

Department of General Surgery, The Second Affiliated Hospital of Soochow University, Suzhou, Jiangsu 215004, People's Republic of China

*These authors contributed equally to this work

Background: Circular RNAs (circRNAs) play an important role in the tumorigenesis of pancreatic cancer. However, the expression profiles and roles of circRNAs in pancreatic cancer remain largely unknown.

Methods: To identify differentially expressed circRNAs (DEcircRNAs) between pancreatic cancer and matched normal tissues, bioinformatics analysis was performed. Hsa_circ_0000069 was identified by 0.bioinformatics analysis. In addition, the level of hsa_circ_0000069 in pancreatic cancer tissues and cell lines, and pancreatic cancer cell-derived exosomes were assessed using RT-qPCR assay.

Results: The expression of hsa_circ_0000069 was markedly upregulated in pancreatic cancer tissues and cell lines. SCL/TAL1 interrupting locus (STIL) is the parent gene for hsa_circ_0000069, and its high expression was related to poor overall survival in patients with pancreatic cancer. In addition, downregulation of hsa_circ_0000069 markedly suppressed STIL expression, induced the apoptosis and cell cycle arrest, and inhibited the proliferation, migration and invasion in pancreatic cancer cells. Moreover, hsa_circ_0000069 knockdown inhibited the growth of xenograft pancreatic cancer tumors in vivo. Furthermore, human pancreatic duct epithelial cells (HPDE) are capable of internalizing SW1990 cell-derived exosomes, allowing the transfer of hsa_circ_0000069. Significantly, SW1990 cell-derived exosomes promoted the proliferation, migration and cell cycle progression of HPDE cells, whereas exosomes with downregulated hsa_circ_0000069 suppressed the proliferation, migration and cell cycle progression of HPDE cells, by suppressing STIL expression.

Conclusion: Our results suggest that hsa_circ_0000069 knockdown could inhibit pancreatic cancer tumorigenesis and exosomes with downregulated hsa_circ_0000069 could suppress HPDE cell malignant transformation. Collectively, hsa_circ_0000069 might be a therapeutic target for the treatment of pancreatic cancer.

Keywords: pancreatic cancer, hsa_circ_0000069, tumorigenesis, exosomes

Correspondence: Wei Chen; Wei Li
Department of General Surgery, The Second Affiliated Hospital of Soochow University, 1055 Sanxiang Road, Suzhou, Jiangsu 215004, People's Republic of China
Email chenwei1971best@126.com; li.wei1@yandex.com

Introduction

Pancreatic cancer is one of the major causes of cancer-related mortality and is the 12th most common cancer in human worldwide.[1,2] The 5-year overall survival rates of pancreatic cancer remain less than 6%, indicating that pancreatic cancer is one of the deadliest forms of cancer.[3] Chronic pancreatitis, smoking, obesity, diabetes

mellitus are several risk factors that seem to be associated with pancreatic cancer.[4] In addition, surgical resection, chemotherapy and radiation are current therapeutic methods for pancreatic cancer.[1] Pancreatic ductal adenocarcinoma (PDAC) is the most common and lethal form of pancreatic cancer, which is considered a highly heterogeneous neoplasm.[5,6] Meanwhile, the average survival time of patients with PDAC is no more than 6 months.[7] However, most patients with pancreatic cancer are diagnosed in the advanced stages, ultimately succumb to metastatic disease.[8] Therefore, identification of promising cancer-associated biomarkers of pancreatic cancer may help to improve the early diagnosis and treatment of pancreatic cancer.

Circular RNAs (circRNAs) are a class of non-coding RNA molecules that form a closed loop structure without 5′ and 3′ ends.[9] CircRNAs participated in the process of transcriptional and post-translational regulations of gene expression.[10] In addition, circRNAs play important roles in human diseases, such as cancer and heart disease.[11,12] Evidences have shown that circRNAs are aberrantly expressed in pancreatic cancer tissues, and participated in tumorigenesis and metastasis in pancreatic cancer.[13,14] However, the role of circRNAs in pancreatic cancer has not been fully clarified.

MicroRNAs (miRNAs) are another class of non-coding RNA molecules (~20 nucleotides) that could downregulate the expression of target genes at post-transcriptional level.[15] In addition, miRNAs may function as oncogenes or tumor suppressors by mediating the expression of their targets in human cancers.[16,17] It has been shown that circRNAs can function as competing endogenous RNA (ceRNA) to regulate expression of downstream target genes.[18]

Exosomes are extracellular vesicles ranging from 30 to 150 nm in diameter.[19] Exosomes contain a specific composition of functional mRNAs, miRNAs, lncRNAs, circRNAs and proteins, playing an important role in cell-to-cell communication via transferring genetic message.[20–22] A recent study has shown that exosomal circRNAs could promote tumor progression.[23] For example, circular RNA IARS can be transported by exosomes from pancreatic cancer cells to endothelial cells, thereby promote tumor progression.[24]

In this study, we identified that hsa_circ_0000069 were significantly upregulated in pancreatic cancer tissues. Further studies indicated that hsa_circ_0000069 might be an important oncogenic regulator involved in pancreatic cancer progression via functioning as a ceRNA for miR-144. In addition, exosomes with downregulated hsa_circ_0000069 were found to be released by pancreatic cancer cells, suppressing the malignant transformation of HPDE cells. These data indicated that hsa_circ_0000069 may be used as a potential biomarker for the diagnosis and therapy of pancreatic cancer.

Materials and Methods

Data Acquisition and Identification of DEcircRNAs

The raw microarray data of pancreatic cancer (GSE69362) were downloaded from the Gene Expression Omnibus database (GEO, https://www.ncbi.nlm.nih.gov/geo/). GSE69362 dataset contains circRNAs expression data of 6 pancreatic cancer tissues and 6 matched normal tissues. R language was applied to identify the DEcircRNAs. DEcircRNAs were identified using an adjusted $P < 0.05$ and a $|\log2(FC)|>2$ as criteria.

Survival Analysis

TCGA dataset (http://tcga-data.nci.nih.gov/tcga) was applied to identify the association between STIL expression and overall survival time. $P < 0.05$ was considered as statistically significant.

Clinical Samples

Thirty pairs of pancreatic cancer tissue samples and adjacent normal tissues were obtained from patients with pancreatic cancer who underwent surgery in the Second Affiliated Hospital of Soochow University, between April 2018 and July 2019. The present study was approved by the Ethics Committee of the Second Affiliated Hospital of Soochow University. Written informed consent was obtained from all patients.

Cell Culture

The pancreatic cancer cell lines, MiaPaCa-2, SW1990, PANC-1 and BXPC3, were obtained from American Type Culture Collection (ATCC, Rockville, MD, USA). Human pancreatic duct epithelial cells (HPDE) were obtained from the Type Culture Collection of the Chinese Academy of Sciences (Shanghai, China). Cells were cultured in Dulbecco's modified Eagle's medium (DMEM, Thermo Fisher Scientific, Waltham, MA, USA) supplemented with 10% fetal bovine serum (FBS, Thermo Fisher Scientific) and 1% penicillin-streptomycin, and incubated in humidified atmosphere containing 5% CO_2 at 37°C.

Lentivirus Production and Cell Transduction

The anti-sense oligonucleotides to suppress hsa_circ_0000069 expression (hsa_circ_0000069 shRNAs) and the oligonucleotides to overexpress hsa_circ_0000069 (hsa_circ_0000069 OE) expression were designed and obtained by Ribobio (Guangdong, China) respectively. 293T cells were transfected with plasmids described above and lentivector packaging plasmids using Lipofectamine2000 (Thermo Fisher Scientific). After that, virus-containing supernatant was collected at 72 h. Subsequently, the viral supernatant was added into MiaPaCa or SW1990 cells. Following 48 h of transduction, the infected cells were selected with puromycin (2 μg/mL, Amresco, Cleveland, OH, USA).

The oligonucleotide sequences were listed as followed: hsa_circ_0000069-shRNA1: 5′- TACTTCAGGCACAGG TCTTTTCAAGAGAAAGACCTGTGCCTGAAGTATT-TTT-3′; hsa_circ_0000069shRNA2: 5′- ACAGGTCTTCC CAAAAGTTTTCAAGAGAAACTTTTGGGAAGACCT-GTTTTTT-3′.

Cell Transfection

MiR-144 agomir, miR-144 antagomir and NC were obtained from GenePharma (Shanghai, China). Later on, miR-144 agomir, miR-144 antagomir, and NC were transfected into SW1990 cells using Lipofectamine 2000 (Thermo Fisher Scientific).

RT-qPCR

Trizol Reagent (Sigma Aldrich, St. Louis, MO, USA) was used to extract total RNA according to the manufacturer's protocol. First strand cDNA was synthesized with EntiLink™ 1st Strand cDNA Synthesis Kit (ELK Biotechnology, Hubei, China). After that, qPCR was performed using SYBR Select Master Mix (Applied Biosystems, Foster City, CA, USA) on a Quantstudio™ DX Real-Time PCR Instrument (Applied Biosystems, Waltham, MA, USA). The sequences of primers were U6, Forward, 5′-C TCGCTTCGGCAGCACAT-3′; Reverse, 5′-AACGCTTCA CGAATTTGCGT-3′. MiR-144, Forward, 5′- ATACTGTAAG CTCAACTGAATTGCC-3′; Reverse, 5′-CTCAACTGGTGT CGTGGAGTC-3′. Actin, Forward, 5′- GTCCACCGCAAAT GCTTCTA-3′; Reverse, 5′-TGCTGTCACCTTCACCGTTC -3′. Hsa_circ_0000069, Forward, 5′- CTACTTCAGGCAC AGGTCTTCC-3′; Reverse, 5′- AAGTTCAGGAACTGAT GGTTGG-3′. Actin was chosen as the internal control for hsa_circ_0000069. U6 was chosen as an internal control for miR-144. The levels of hsa_circ_0000069, miR-144 were calculated using the 2-ΔΔCt method.

CCK-8 Assay

Cell viability was measured using the Cell Counting Kit-8 (CCK-8, Beyotime, Shanghai, China) according to the manufacturer's protocols. MiaPaCa-2, SW1990 and PANC-1 cells were seed onto 96-well plates at a density of 5000 cells per well, and treated with 10 μL of CCK-8 solution. Then, the absorbance was measured at a wavelength of 450 nm using a microplate reader (BioTek, Winooski, VT, USA).

EdU Staining Assay

A Click-iT™ EdU Cell Proliferation Kit (Thermo Fisher Scientific) was used to determine the proliferation of pancreatic cancer cells according to the manufacturers' protocols. Cells were observed with a fluorescence microscope (Olympus, Tokyo, Japan). Nuclei were counterstained with DAPI.

Dual-Luciferase Reporter Assay

The hsa_circ_0000069 (wild type) and its mutant sequences were inserted into pmirGLO luciferase reporter vectors (Promega, Madison, WI, USA). Then, wild type (WT)-hsa _circ_0000069 or mutant (MT)-hsa_circ_0000069 plasmid was co-transfected with miR-144 agomir and NC, respectively, using Lipofectamine 2000 in SW1990 cells for 48 h. The STIL (WT) and its mutant sequences were inserted into pmirGLO luciferase reporter vectors. Then, WT-STIL or MT-STIL plasmid was co-transfected with miR-144 agomir and NC, respectively, using Lipofectamine 2000 in SW1990 cells for 48 h. Later on, luciferase activities were measured by using the Dual-Luciferase Reporter Assay System (Promega, Madison, USA) with renilla luciferase activity as endogenous control.

RNA Pull-Down

RNA pull-down was performed using Magnetic RNA-protein Pull-down Kit (Thermo Fisher Scientific) according to the manufacturer's protocols. SW1990 cells were transfected with biotinylated hsa_circ_0000069 for 24 h. After that, streptavidin-coated magnetic beads were added into cells and incubated for 30 min at room temperature. Later on, the biotin-coupled RNA complex was pulled down. Subsequently, the abundance of miR-144 in bound fractions was conducted by RT-qPCR.

Fluorescence in situ Hybridization (FISH) Analysis

The oligonucleotide probe for hsa_circ_0000069 was designed and synthesized from Ribobio (Guangzhou, China). FISH assay was performed using Ribo™ Fluorescent in Situ Hybridization Kit (Ribobio Company, China) as described in previous study.[25] A confocal laser-scanning microscope (Leica, Buffalo Grove, IL, USA) was used to capture the images.

Transwell Invasion Assay

Cell invasion was analyzed using 24-well transwell chambers (0.8 μm; Corning New York, NY, USA) with Matrigel coating. 4 x 10^4 MiaPaCa-2 and SW1990 cells in 200 μL serum-free medium were seed onto the upper chamber. After that, the lower chamber contained 600 μL of DMEM medium plus 10% FBS, which acted as a chemoattractant. After 24 h of incubation, the cells that invade from the upper part of the filter to the lower part were fixed with 4% paraformaldehyde, and then stained with 0.2% crystal violet. Subsequently, the invaded cells were photographed using a fluorescence microscope (Olympus, Tokyo, Japan).

Wound Healing Assay

MiaPaCa-2 and SW1990 cells were seeded onto 6-well culture plate at a density of 2×10^5 cells per well overnight. When the cells were cultured to 90% confluence, a wound was made using a sterile 200 μL pipette tip. After that, the cells were washed twice with PBS, and then infected with hsa_circ_0000069-shRNA2 for 48 h. The width of the wound area was photographed at 0 h and 48 h after scratching using a microscope.

Flow Cytometry

For the cell apoptosis assay, the percentage of apoptotic cells was examined by using an Annexin V-FITC Apoptosis Detection kit (Thermo Fisher Scientific) in a flow cytometer (FACScan™, BD Biosciences, Franklin Lakes, NJ, USA).

For the cell cycle assay, SW1990 cells were washed twice with pre-cooling PBS, and then stained with PI/RNase Staining Buffer (BD Biosciences, San Jose, CA, USA). After that, cell cycle distribution was analyzed using a flow cytometer (BD Biosciences).

Western Blot Assay

MiaPaCa-2 and SW1990 cells were lysed in RIPA lysis buffer. After that, proteins were subjected to 10% SDS-PAG, and then electrotransferred onto a PVDF membrane (Millipore, Billerica, MA, USA). Later on, the membrane was blocked with 5% skim milk in TBST for 1 h, and then incubated with primary antibodies overnight at 4°C. Antibodies were diluted to 1:1000 for active caspase 3 (Abcam Cambridge, MA, USA), STIL (Abcam), GLi1 (Abcam), CDK1 (Abcam), Cyclin B1 (Abcam), β-actin (Abcam). Subsequently, the membrane was incubated with HRP-conjugated secondary antibody (Abcam) at room temperature for 1 h, and the blots were visualized by an enhanced chemiluminescent substrate kit (Thermo Fisher Scientific).

Exosome Isolation and Identification

Exosomes were collected from the conditioned medium of HPDE and SW1990 cells and isolated by ultracentrifugation as described previously.[26] Exosomes were resuspended in PBS and stored at −80°C until usage. The size and concentration of the exosomes were analyzed by a nanoparticle tracking analysis (NTA) instrument (ZetaView, Particle Metrix, Meerbusch, Germany). The morphology of exosomes was observed using a transmission electron microscopy (TEM, StarJoy, Japan; JSM-7800F). After that, protein concentration in exosomes was detected by BCA method after lysis of the exosomes. Later on, the surface markers of the exosomes, TSG101, CD63, CD9 and CD81, were analyzed by Western blot assay. Monoclonal rabbit anti-TSG101, anti-CD63, anti-CD9 and anti-CD81 antibodies were purchased from Abcam Cambridge.

Exosomes Tracing

The isolated exosomes were labeled with the PKH26 red fluorescent dye (Sigma Aldrich, St. Louis, MO, USA) and incubated at 37°C for 30 min. Later on, the HPDE cells were incubated with labeled exosomes for 24 h at 37°C. After that, the cytoskeleton of HPDE cells was stained with phalloidin-FITC (green), and cell nuclei was stained with DAPI (blue). Subsequently, the internalization of exosomes by HPDE cells was measured by a confocal microscope (Carl Zeiss, Jena, Germany).

Animal Study

BALB/c nude mice (6–8 weeks old) were obtained from the Vital River Laboratories (Beijing, China). All animal

experiments were approved by the Ethics Committee of the Second Affiliated Hospital of Soochow University (NO. SC2019101513). Animals were randomized into three groups: blank, NC and has_circ_0000069-shRNA2 group. 5 x 10^6 SW1990 cells or SW1990 cells stably expressing shRNA-NC, has_circ_0000069-shRNA2 in 100 μL PBS were injected into the left flank of nude mice. The tumor volume was measured every week by the following formula V = (length x width^2)/2. After 4 weeks, animals were killed by following the recommended procedures of National Institutes of Health guide for the care and use of laboratory animals, and the weight of the tumors was measured.

TUNEL Staining Assay

Paraffin-embedded tumor tissues were cut into 3 μm slices. After that, deparaffinized tissue sections were stained using an APO-BrdU™ TUNEL Assay Kit (Thermo Fisher Scientific) according to the manufacturer's protocols.

Statistical Analysis

Data are presented as the mean ± standard deviation (S. D.). All statistical analyses were performed using GraphPad Prism software (version 7.0, La Jolla, CA, USA). All figures were produced using GraphPad Prism software. One-way analysis of variance (ANOVA) and Tukey's tests were carried out for multiple group comparisons. All data were repeated in triplicate. The differences were considered significant at *P < 0.05.

Results

Identification of DEcircRNAs in Pancreatic Cancer

Raw data from GSE69362 were downloaded from GEO database, DEcircRNAs were identified by R package. Hierarchical clustering analysis revealed circRNA expression patterns that differed between pancreatic cancer and matched normal tissues (Figure 1A). A total of 154 DEcircRNAs (60 down- and 94 upregulated circRNAs) were screened from the GSE69362 dataset, and the distribution of DEcircRNAs was presented by volcano plot (Figure 1B). TCGA data revealed that hsa_circ_0000069 levels in 179 pancreatic cancer tissues were higher than that of in 171 normal tissues (Figure 1C). In addition, STIL is the parent gene of hsa_circ_0000069, high levels of STIL correlated with poor overall survival rates in patients with pancreatic cancer (Figure 1D).

The Expression of Hsa_circ_0000069 in Pancreatic Cancer and Normal Tissues

As shown in Figure 1E, the level of hsa_circ_0000069 was significantly increased in tumor tissues compared with normal tissues. In addition, the diagnostic value of hsa_circ_0000069 expression in pancreatic cancer tissues was assessed by receiver operating characteristic (ROC) curve analysis (Figure 1F). The area under the ROC curve was 0.8944, which indicated diagnostic value. Meanwhile, as shown in Table 1, hsa_circ_0000069 correlated with clinicopathological parameters such as the distant metastasis and tumor volume. These results indicated that hsa_circ_0000069 is upregulated in pancreatic cancer and is associated with a poor prognosis.

Downregulation of Hsa_circ_0000069 Inhibited the Proliferation of Pancreatic Cancer Cells

To determine the role of hsa_circ_0000069 in pancreatic cancer cells, we analyzed hsa_circ_0000069 levels in one human pancreatic duct epithelial cell line HPDE, and four pancreatic cancer cell lines SW1990, MiaPaCa, PANC-1 and BXPC3, by using RT-qPCR. We found that hsa_circ_0000069 level was notably upregulated in SW1990, MiaPaCa and PANC-1 cells, compared with HPDE cells (Figure 2A). Thus, SW1990, MiaPaCa, PANC-1 cells were utilized in the following studies. Next, we used two shRNAs (hsa_circ_0000069 shRNA1, hsa_circ_0000069 shRNA2) to downregulate hsa_circ_0000069 in MiaPaCa-2 and SW1990 cells. RT-qPCR assay results confirmed significant downregulation of hsa_circ_0000069 after infection with hsa_circ_0000069 shRNAs (Figure 2B and C). Hsa_circ_0000069 shRNA2 downregulated hsa_circ_0000069 more markedly than hsa_circ_0000069 shRNA1 in MiaPaCa-2 and SW1990 cells, thus, hsa_circ_0000069 shRNA2 plasmid was utilized in the following experiments (Figure 2B and C). In addition, the results of CCK-8 assay indicated that downregulation of hsa_circ_0000069 notably inhibited the viability of MiaPaCa-2, SW1990 and PANC-1 cells (Figures 2D and E, and Supplementary Figure 1A). Moreover, the results of EdU staining assay showed that downregulation of hsa_circ_0000069 notably inhibited the proliferation of MiaPaCa-2 and SW1990 cells (Figure 2F

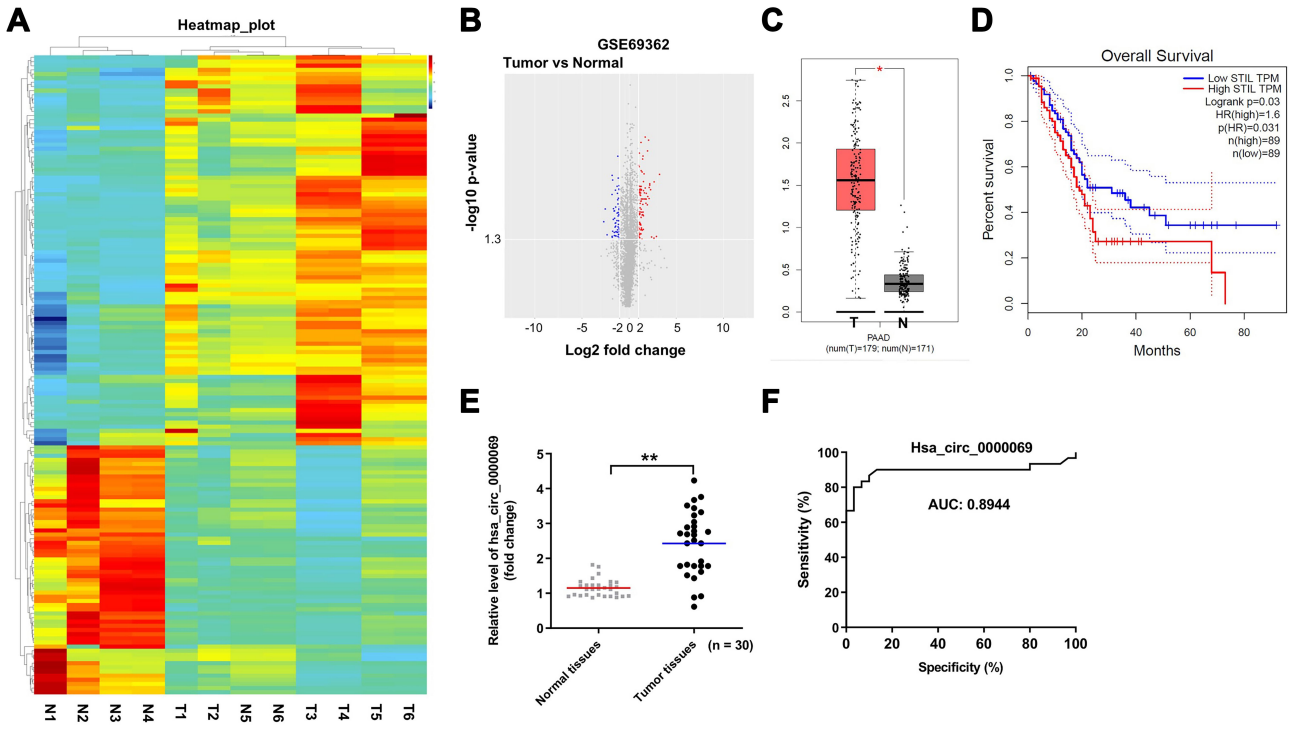

Figure 1 The expression of hsa_circ_0000069 in pancreatic cancer and normal tissues. (**A**) The heatmaps of the DEcircRNAs profiles in pancreatic cancer tissues (T group) and normal controls (N group) in GSE69362. (**B**) Volcano plot of DEcircRNAs in GSE69362. Blue and red color represent relatively low and high expression of circRNAs in the corresponding group respectively. -log10 p-value > 1.3 and |log2 Fold Change| > 2 were set as the threshold. (**C**) Relative expression of hsa_circ_0000069 level in pancreatic cancer tissues (n = 179, T) and in normal tissues (n = 171, N) in TCGA dataset. *P < 0.05. (**D**) Survival analysis of the correlation between STIL levels and survival rates in NSCLC patients. (**E**) The relative expression of hsa_circ_0000069 in the tumor tissues and adjacent normal tissues of patients with pancreatic cancer (n = 30). **P < 0.01. (**F**) The ROC curves were applied for evaluating the diagnostic value of hsa_circ_0000069.

and G). These data suggested that knockdown of hsa_circ_0000069 could inhibit the proliferation of pancreatic cancer cells.

Table 1 The Correlation of Hsa_circ_0000069 with Clinic-Pathological Parameters of Patients with Pancreatic Cancer

Parameters	Number	hsa_circ_0000069	*p* value
Age			0.334
≤ 50	12	2.23 ± 0.61	
> 50	18	3.03 ± 0.63	
Tumor volume			
≤ 2 cm	17	3.03 ± 0.63	0.041*
> 2 cm	13	2.23 ± 0.61	
Gender			0.261
Male	15	2.24 ± 0.79	
Female	15	2.62 ± 0.99	
Distant metastasis			0.046**
Yes	17	2.72 ± 0.93	
No	13	2.05 ± 0.73	
TNM stage			0.739
I–II	12	2.47 ± 0.83	
III–IV	18	2.36 ± 1.02	

Notes: Student's *t*-test, *P<0.05; **P<0.01.

Hsa_circ_0000069 Functions as a ceRNA of miR-144 in SW1990 Cells

Circular RNA interactome (https://circinteractome.nia.nih.gov) was used to predict potential miRNAs interacted with hsa_circ_0000069. According to the analysis, miR-144 had a complementary sequence to hsa_circ_0000069 (Figure 3A). As indicated in Figure 3B, miR-144 agomir significantly increased the level of miR-144 in SW1990 cells, and miR-144 antagomir markedly decreased the level of miR-144 in SW1990 cells. In addition, the results of dual-luciferase reporter assay indicated that overexpression of miR-144 led to a marked decrease in luciferase activity of the wild-type hsa_circ_0000069 vector in SW1990 cells (Figure 3C). Meanwhile, RNA pull-down assay with biotinylated hsa_circ_0000069 found that miR-144 was pulled down by biotin-labeled hsa_circ_0000069, indicating miR-144 directly binds to hsa_circ_0000069 (Figure 3D). Meanwhile, FISH assay indicated that hsa_circ_0000069 and miR-144 were partially co-localized in the cytoplasm, suggesting the direct interaction of hsa_circ_0000069 with miR-144 (Figure 3E). The results above indicated that hsa_circ_0000069 could act as a sponge for miR-144.

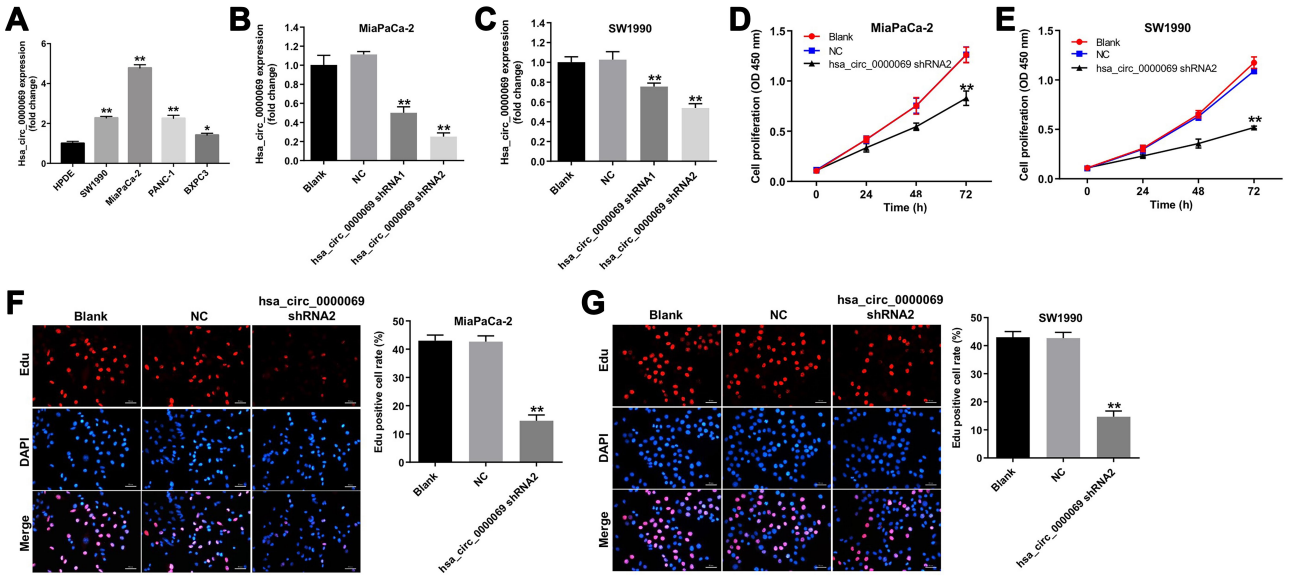

Figure 2 Downregulation of hsa_circ_0000069 inhibited the proliferation of pancreatic cancer cells. (**A**) Hsa_circ_0000069 levels in one human pancreatic duct epithelial cell line HPDE, and four pancreatic cancer cell lines SW1990, MiaPaCa, PANC-1 and BXPC3 were detected by RT-qPCR. (**B**) MiaPaCa and (**C**) SW1990 cells were infected with hsa_circ_0000069 shRNA1 or hsa_circ_0000069 shRNA2 for 72 h. The level of hsa_circ_0000069 in MiaPaCa and SW1990 cells was analyzed by RT-qPCR. (**D**) MiaPaCa and (**E**) SW1990 cells were infected with hsa_circ_0000069 shRNA2 for 24, 48 and 72 h. Cell viability was analyzed by CCK-8 assay. (**F** and **G**) Cell proliferation was detected by EdU assay. *P < 0.05, **P < 0.01 compared with NC group.

Downregulation of Hsa_circ_0000069 Inhibited the Migration and Invasion and Induced the Apoptosis of Pancreatic Cancer Cells via miR-144

To investigate the role of hsa_circ_0000069 on invasion and migration of pancreatic cancer cells, transwell invasion assay and wound healing assay were performed. As shown in Figures 4A–D, and Supplementary Figure 1B and C, downregulation of hsa_circ_0000069 obviously suppressed the invasive and migratory abilities of MiaPaCa, SW1990 and PANC-1 cells; however, these changes were reversed by miR-144 knockdown. In addition, knockdown of hsa_circ_0000069 markedly induced the apoptosis of MiaPaCa, SW1990 and PANC-1 cells; but, that effect was reversed by miR-144 knockdown (Figures 4E and F, and Supplementary Figure 1D). Moreover, knockdown of hsa_circ_0000069 led to increased expression of active caspase 3 protein in MiaPaCa and SW1990 cells (Figure 4G and H). However, addition of miR-144 antagomir reversed the effect of hsa_circ_0000069 shRNA2 on the expression of active caspase 3 in MiaPaCa and SW1990 cells (Figure 4G and H). These data illustrated that downregulation of hsa_circ_0000069 could suppress the migration and invasion, and induce the apoptosis in pancreatic cancer cells via miR-144.

Downregulation of Hsa_circ_0000069 Inhibited the Growth of Pancreatic Cancer Cells by Targeting miR-144/STIL Axis

The 3′-UTR of STIL has the same binding sites that hsa_circ_0000069 combined with miR-144 (Figure 5A). In addition, the dual-luciferase reporter assay verified that miR-144 agomir significantly inhibited the luciferase activity of the wild-type STIL 3′UTR vector (Figure 5B). These data indicated that STIL was a binding target of miR-144. Moreover, downregulation of hsa_circ_0000069 notably decreased the expressions of STIL, GLi1, CDK1, cyclin B1 in SW1990 cells; however, these changes were reversed by miR-144 knockdown (Figure 5C and D). Meanwhile, the results of cell cycle assay indicated that SW1990 cells with stable knockdown of hsa_circ_0000069 displayed a significant decrease in the percentages of cell in S phase but increased proportions in G2-M phase cells, compared with NC group; however, these changes were reversed by miR-144 knockdown (Figure 5E). These results illustrated that downregulation of hsa_circ_0000069 could inhibit the growth of pancreatic cancer cells by targeting miR-144/STIL axis.

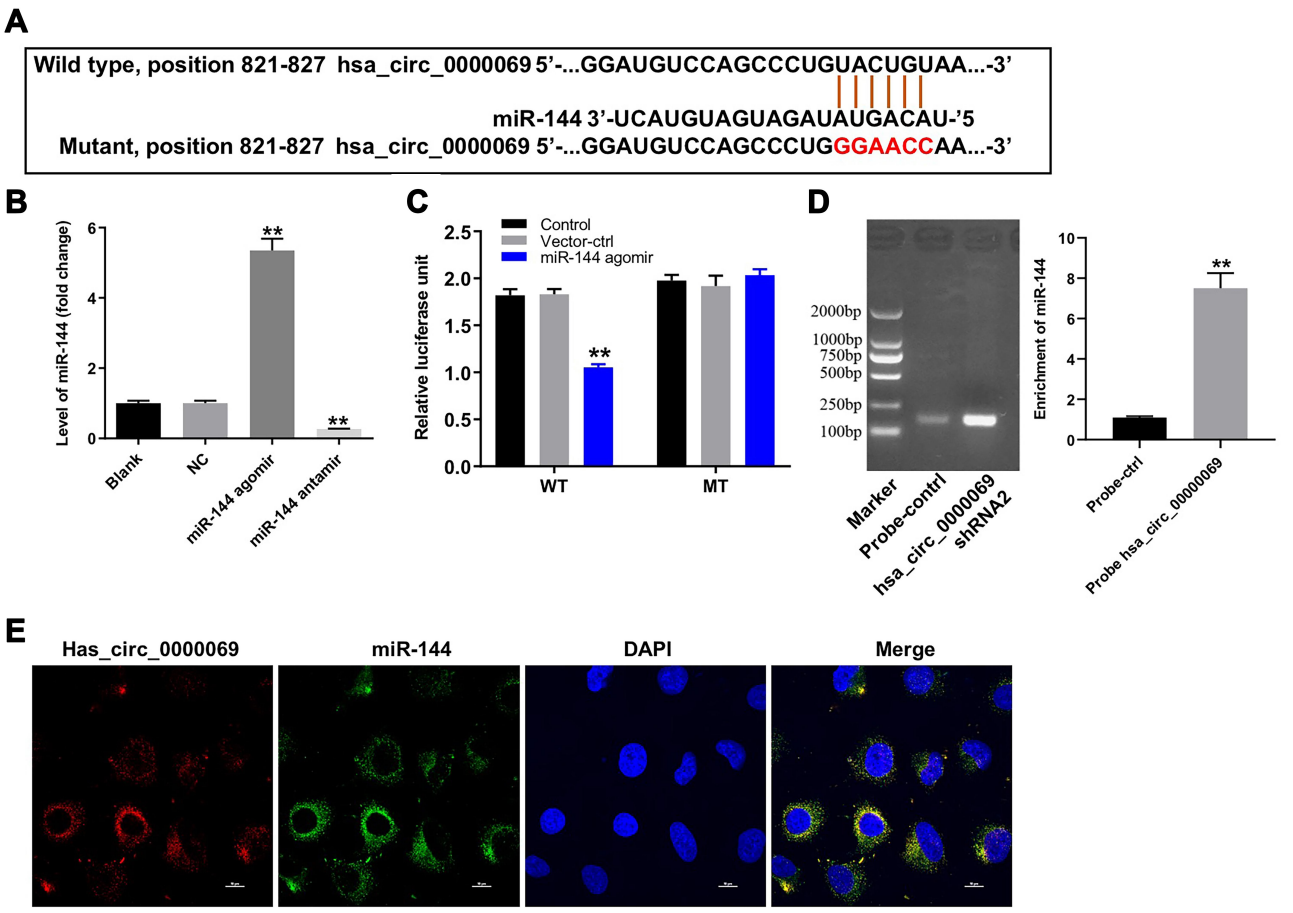

Figure 3 Hsa_circ_0000069 functions as a ceRNA of miR-144 in SW1990 cells. (**A**) The putative binding sites of miR-144 on hsa_circ_0000069, and target sequences were mutated. (**B**) The level of miR-144 in SW1990 cells transfected with miR-144 agomir or miR-144 antagomir was detected by RT-qPCR respectively. **P < 0.01 compared with NC group. (**C**) Luciferase assay of SW1990 cells transfected with hsa_circ_0000069-WT or hsa_circ_0000069-MT reporter together with miR-144 or NC. **P < 0.01 compared with vector-control group. (**D**) SW1990 cells transfected with biotin-labeled hsa_circ_0000069, assayed by biotin based pull down. MiR-144 levels were analyzed by RT-qPCR. **P < 0.01 compared with probe-control group. (**E**) The cellular localization of hsa_circ_0000069 and miR-144 in SW1990 cells was analyzed using FISH assay.

Exosomal Transfer of Hsa_circ_0000069 from SW1990 Cells to HPDE Cells

Evidences have been shown that circRNAs can be secreted and delivered via exosomes into recipient cells.[23,27] In addition, exosomal circRNAs can promote tumor cell proliferation and migration.[24] In order to investigate whether exosomal hsa_circ_0000069 performs the above functions, we first extracted exosomes from the HPDE and SW1990 cells. The size and number of the isolated exosomes, as well as their morphology were identified by NTA analysis and TEM. The data showed that the exosomes from both HPDE and SW1990 cells were approximately 100 nm in diameter, and exhibited a cup-shaped morphology (Figure 6A–D). Moreover, the presence of exosomal markers TSG101, CD63, CD9, CD81 was identified using Western blotting analysis (Figure 6E). These data indicated that exosomes were successfully isolated from HPDE and SW1990 cells. Meanwhile, RT-qPCR assay indicated that exosomal hsa_circ_0000069 was found to be upregulated in the supernatants of SW1990 cells, rather than HPDE cells (Figure 6F).

Wei et al found that exosomal miR-15b-3p was found to be secreted by gastric cancer cells, promoting malignant transformation of gastric mucosa epithelium cells.[28] We then focused on whether exosomal hsa_circ_0000069 involved in the communication between SW1990 cells and HPDE cells. To determine whether SW1990 cell-derived exosomes were internalized by HPDE cells, the exosomes were labeled with PKH26 and incubated with HPDE cells. After 24 h of co-cultivation, PKH26-labeled exosomes (red fluorescence) were observed in most HPDE cells (Figure 6G). Next, in order to determine the exosome-mediated intercellular circRNA transfer, exosomes derived from hsa_circ_0000069-overexpressing or hsa_circ_0000069-knockdown SW1990 cells were co-cultured

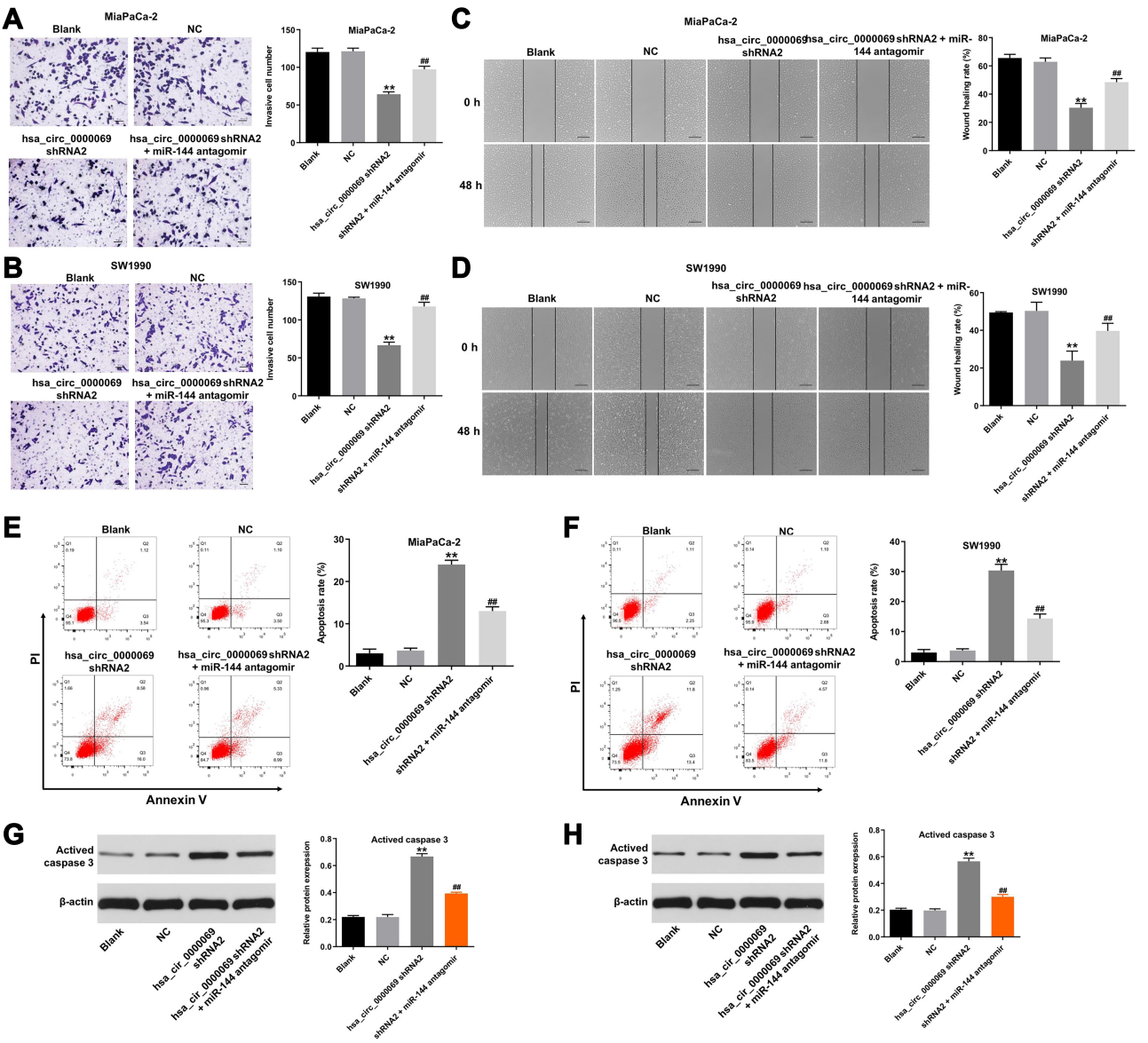

Figure 4 Downregulation of hsa_circ_0000069 inhibited the migration and invasion, and induced the apoptosis of pancreatic cancer cells via miR-144. (**A**) MiaPaCa and (**B**) SW1990 cells were transfected with hsa_circ_0000069 shRNA2 with or without miR-144 antagomir for 24 h. The invasion ability of MiaPaCa and SW1990 cells was measured using transwell invasion assay. (**C**) MiaPaCa and (**D**) SW1990 cells were transfected with hsa_circ_0000069 shRNA2 with or without miR-144 antagomir for 48 h. The migration ability of MiaPaCa and SW1990 cells was measured using wound healing assay. (**E** and **F**) MiaPaCa and SW1990 cells were transfected with hsa_circ_0000069 shRNA2 with or without miR-144 antagomir for 72 h. Apoptotic cells were detected with Annexin V and PI double staining. (**G** and **H**) Expression level of active caspase 3 in MiaPaCa and SW1990 cells was detected with Western blotting and quantified via normalization to β-actin. **P < 0.01 compared with NC group; ##P < 0.01 compared with hsa_circ_0000069 shRNA2 group.

with HPDE cells for 24 h. We then characterized the exosomes using Western blotting for the exosomal markers TSG101, CD63, CD9 and CD81 (Figure 6H). In addition, RT-qPCR assay showed that hsa_circ_0000069 level in HPDE cells was significantly increased in HPDE cells co-cultured with SW1990 cell-derived exosomes with hsa_circ_0000069 overexpression, while being decreased in HPDE cells co-cultured with SW1990 cell-derived exosomes with hsa_circ_0000069 knockdown (Figure 6I). These data indicated that SW1990 cell-derived exosomes can deliver hsa_circ_0000069 to HPDE cells.

Exosomes Derived from Hsa_circ_0000069-Knockdown SW1990 Cells Suppress Malignant Transformation of HPDE Cells

To further investigate the role of SW1990 cell-derived exosomes in recipient cells, CCK-8 assay was applied.

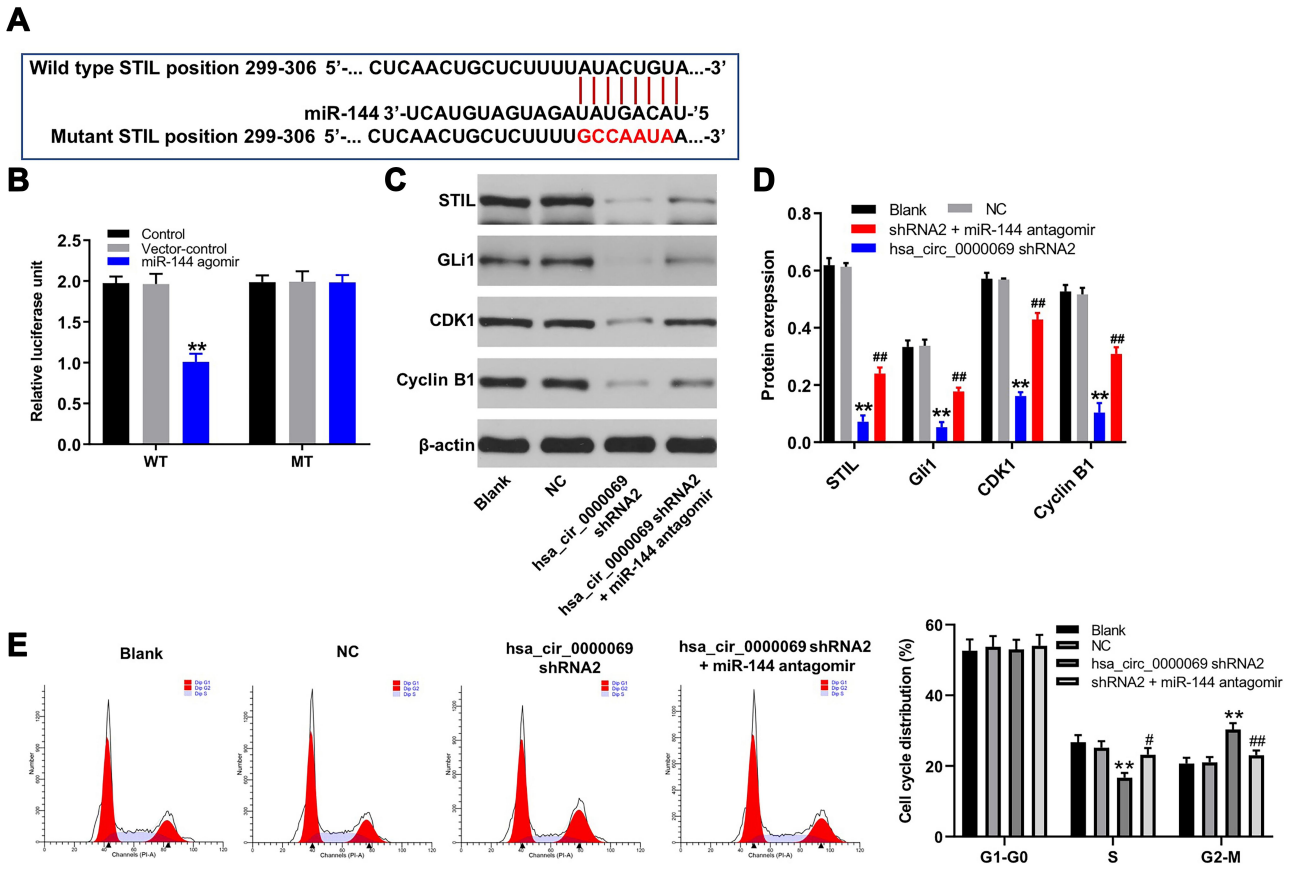

Figure 5 Downregulation of hsa_circ_0000069 inhibited the growth of pancreatic cancer cells by targeting miR-144/STIL axis. (**A**) The putative binding sites of miR-144 on STIL, and target sequences were mutated. (**B**) Luciferase assay of SW1990 cells transfected with STIL-WT or STIL-MT reporter together with miR-144 or NC. **P < 0.01 compared with vector-control group. (**C**) MiaPaCa and SW1990 cells were transfected with hsa_circ_0000069 shRNA2 with or without miR-144 antagomir for 72 h. Expression levels of STIL, GLi1, CDK1, Cyclin B1 in SW1990 cells were detected with Western blotting. (**D**) The relative expressions of STIL, GLi1, CDK1, Cyclin B1 in SW1990 cells were quantified via normalization to β-actin. (**E**) The cell cycle distribution of SW19900 cells was determined by PI staining and flow cytometry. **P < 0.01 compared with NC group; $^{\#}$P < 0.05, $^{\#\#}$P < 0.01 compared with hsa_circ_0000069 shRNA2 group.

As shown in Figure 7A, SW1990 cell-derived exosomes significantly increased the proliferation of HPDE cells; however, when HPDE cells were treated with exosomes with downregulated hsa_circ_0000069, decreased cell proliferation was observed. In addition, the results of wound healing assay indicated that HPDE cells treated with control exosomes (Exo-NC) showed greater migratory capacity than those treated with PBS; however, the migration of HPDE cells was notably inhibited by the exosomes derived from hsa_circ_0000069-knockdown SW1990 cells compared to those derived from control SW1990 cells (Figure 7B). Moreover, HPDE cells treated with exosomes with downregulated hsa_circ_0000069 showed greater apoptotic effect than those treated with Exo-NC (Figure 7C). Meanwhile, HPDE cells treated with exosomes with downregulated hsa_circ_0000069 displayed a significant decrease in the percentages of cells in S-phase but increased proportions in G2/M-phase cells, compared with Exo-NC group (Figure 7D). At the protein level, the expressions of STIL and GLi1 were notably increased in HPDE cells treated with Exo-NC; however, these levels were reversed by the exosomes with downregulated hsa_circ_0000069 (Figure 7E). These data indicated that exosomes derived from hsa_circ_0000069-knockdown SW1990 cells could suppress malignant transformation of HPDE cells.

Downregulation of Hsa_circ_0000069 Inhibited the Growth of Implanted SW1990 Tumors in vivo

To explore the role of hsa_circ_0000069 on tumor growth in vivo, a SW1990 subcutaneous xenograft model was established. As shown in Figure 8A and B, downregulation of hsa_circ_0000069 significantly inhibited tumor volume and tumor weight, compared with NC group. In addition,

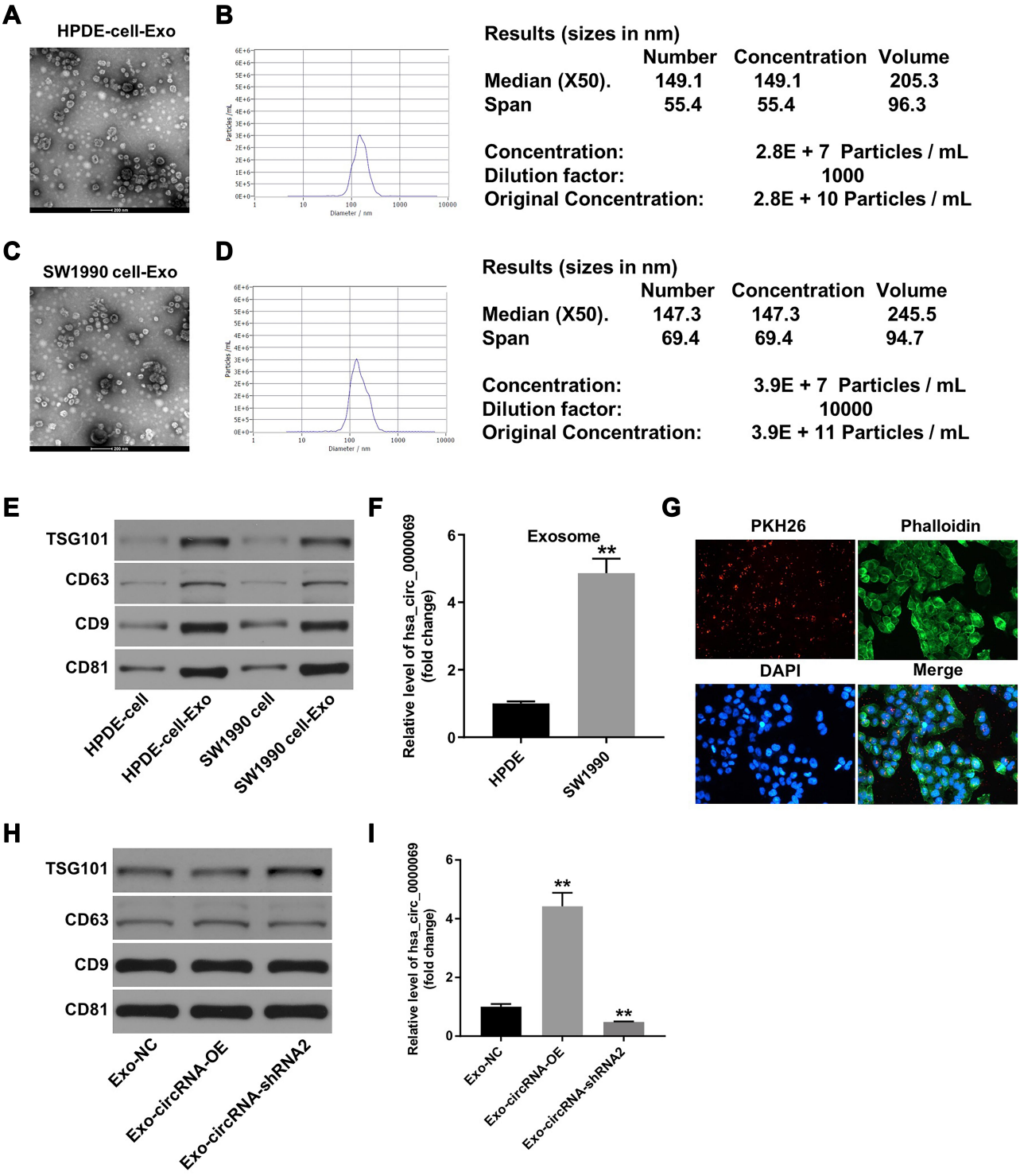

Figure 6 Exosomal transfer of hsa_circ_0000069 from SW1990 cells to HPDE cells. (**A**–**D**) TEM of HPDE and SW1990 cell conditioned medium secreted exosomes. The mean diameter of exosomes was analyzed using the NTA. (**E**) Western blot analysis of exosome surface markers (TSG101, CD63, CD9 and CD81) expressions in exosomes from HPDE and SW1990 cells. (**F**) Relative expressions of exosomal hsa_circ_0000069 in culture supernatant of HPDE and SW1990 cells. **P < 0.01 compared with HPDE group (**G**) Confocal microscopy analysis of the internalization of PKH26-labeled exosomes (red) in HPDE cells. DAPI (blue) was used for nuclei staining, and phalloidin-FITC (green) was used for F-actin staining. (**H**) Exosomes were isolated from hsa_circ_0000069-overexpressing or hsa_circ_0000069-knockdown SW1990 cells. Western blot analysis of exosome surface markers (TSG101, CD63, CD9 and CD81) expressions in exosomes. (**I**) Exosomes (10 μg/mL) derived from hsa_circ_0000069-overexpressing or hsa_circ_0000069-knockdown SW1990 cells were co-cultured with HPDE cells for 24 h. RT-qPCR was used to analyze the efficiency of exosomes in transferring hsa_circ_0000069 to HPDE cells. **P < 0.01 compared with Exo-NC group.

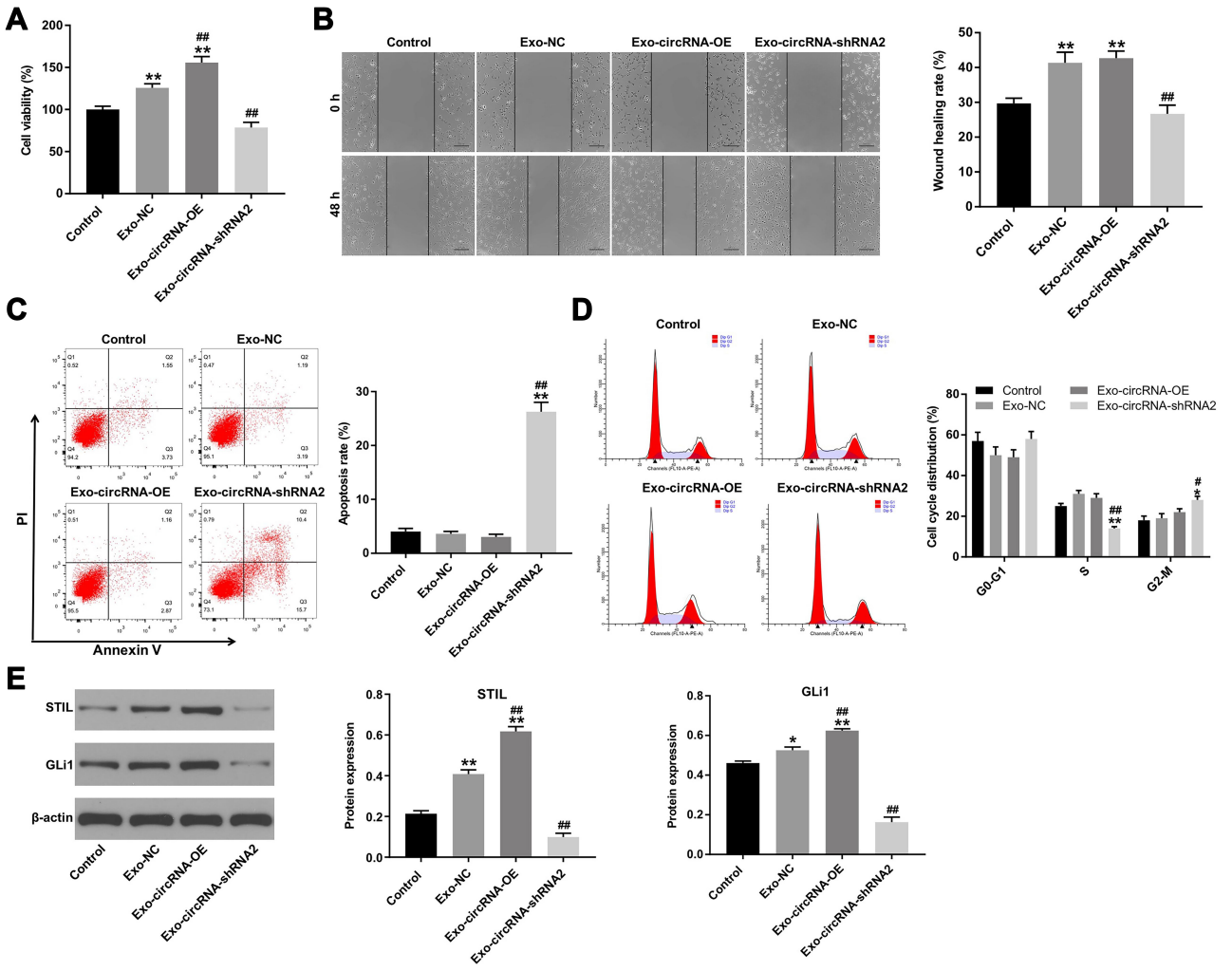

Figure 7 Exosomes derived from hsa_circ_0000069-knockdown SW1990 cells suppress malignant transformation in vitro. Exosomes (10 μg/mL) derived from hsa_circ_0000069-overexpressing or hsa_circ_0000069-knockdown SW1990 cells were co-cultured with HPDE cells for 24 h. (**A**) Cell viability was analyzed by CCK-8 assay. (**B**) The migration ability of HPDE cells was measured using wound healing assay. (**C**) Apoptotic cells were detected with Annexin V and PI double staining. (**D**) The cell cycle distribution of HPDE cells was determined by PI staining and flow cytometry. (**E**) Expression levels of STIL and GLi1 in HPDE cells were detected with Western blotting. *P < 0.05, **P < 0.01 compared with control group; #P < 0.05, ##P < 0.01 compared with Exo-NC group.

downregulation of hsa_circ_0000069 markedly decreased the expressions of STIL and GLi1 in tumor tissues, compared with NC group (Figure 8C and D). Moreover, TUNEL assay illustrated that downregulation of hsa_circ_0000069 markedly induced apoptosis in tumor tissues, compared with NC group (Figure 8E and F). These data indicated that downregulation of hsa_circ_0000069 could inhibit the growth of implanted SW1990 tumors in vivo.

Discussion

The present study profiled circRNA expression pattern in pancreatic cancer and matched normal tissues, and found 154 circRNAs that changed notably during the progression of pancreatic cancer. We screened out the hsa_circ_0000069, which was highly expressed in pancreatic cancer tissues. Following further validation in TCGA dataset, it was identified that high STIL (parent gene of hsa_circ_0000069) expression was associated with poor overall survival rates in patients with pancreatic cancer. To the best of our knowledge, this was the first research on upregulated hsa_circ_0000069 expression in pancreatic cancer, which extended previous studies of other circRNAs.[10,24,29] Further research revealed that downregulation of hsa_circ_0000069 significantly inhibited the proliferation, migration and invasion, as well as induced apoptosis in pancreatic cancer cells. In addition, knockdown of hsa_circ_0000069 markedly suppressed the growth of pancreatic cancer cells in vivo. Thus, hsa_circ_0000069 might function as an oncogene in the development of pancreatic cancer.

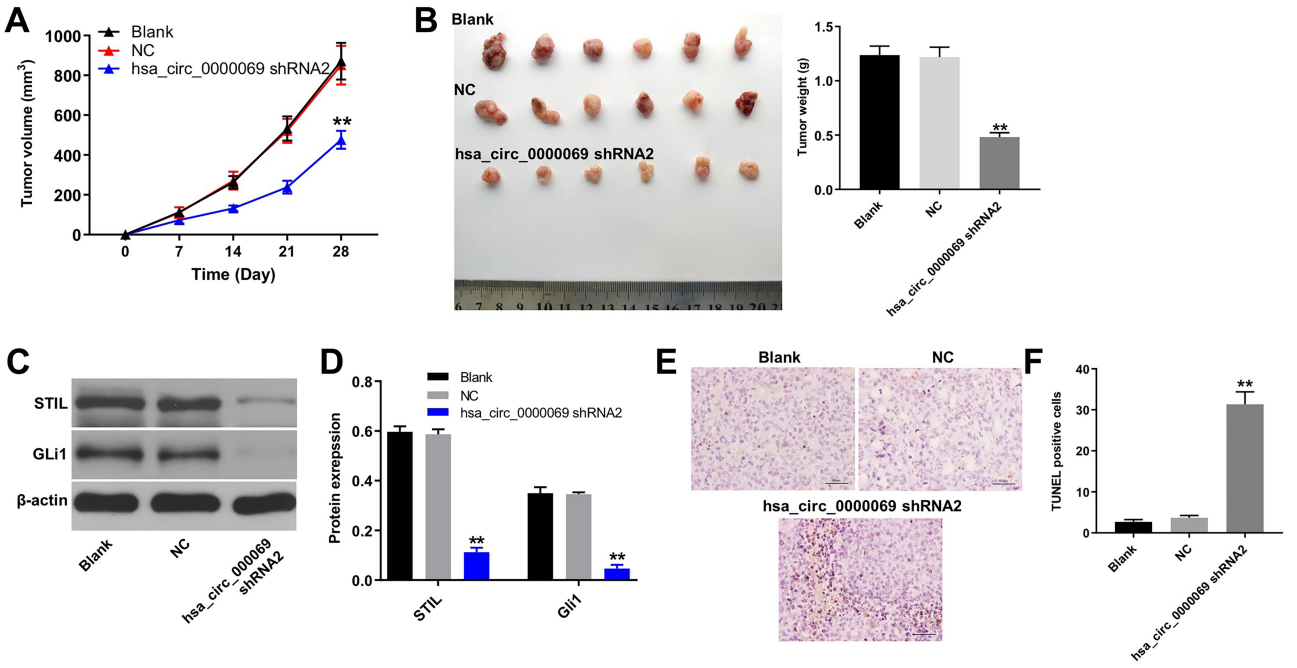

Figure 8 Downregulation of hsa_circ_0000069 inhibited the growth of implanted SW1990 tumors in vivo. (**A**) Xenograft tumor volume of each animal was monitored weekly. (**B**) Xenografts tumors were photographed and calculated. (**C**) Expression levels of STIL, GLi1 in tumor tissues were detected with Western blotting. (**D**) The relative expressions of STIL, GLi1 in tumor tissues were quantified via normalization to β-actin. (**E** and **F**) TUNEL assay of apoptosis in tumor tissues. **P < 0.01 compared with NC group.

Most circRNAs were reported to function as a ceRNA to sponge several miRNAs and suppress their activity.[30] CircRNAs via sponging the miRNAs could enhance the expression of the miRNA-targeted genes.[31] For example, circRNA-5692 can sponge miR-328-5p to enhance DAB2IP expression and the proliferation of hepatocellular carcinoma cells.[32] Circular RNA ACVR2A acts as a sponge of miR-626 to inhibit the proliferation and metastasis of bladder cancer cells.[33] In this study, we verified that hsa_circ_0000069 could interact with miR-144 in pancreatic cancer cells by FISH and RNA pull-down assays. In addition, downregulation of miR-144 could reverse the inhibitory effect of hsa_circ_0000069 knockdown on cell invasion in pancreatic cancer cell lines. These results suggested that hsa_circ_0000069 could serve as a miRNA sponge for miR-144. Our findings may provide novel insights into the role of hsa_circ_0000069 on the circRNA/miRNA regulatory network to mediate the progression of pancreatic cancer.

We further found that miR-144 targeted the STIL because miR-144 overexpression mitigated the STIL-regulated luciferase activity. STIL is the main regulator of mitotic centrosome to promote cell cycling.[34,35] Erez et al found that downregulation of STIL in cancer cells delayed entrance into mitosis, and inhibited activation of the CDK1-cyclin B complex.[36] In this study, we found that hsa_circ_0000069 knockdown markedly decreased the expression of STIL, CDK1 and cyclin B1 in pancreatic cancers, indicating that downregulation of hsa_circ_0000069 could induce cell cycle arrest at the G2M phase in pancreatic cancer cells.

Moreover, we detected the expression of GLI family zinc finger-1 (Gli1). Evidence has shown that STIL can regulate the transcription of Gli1.[37,38] Yu et al revealed that overexpression of Gli1 could promote the progression of pancreatic cancer.[39] Gli1 forms heterodimers with cytoplasmic SUFU protein, while the heterodimers cannot be translocated from the cytoplasm to the nucleus.[37] Interestingly, STIL can bind cytoplasmic SUFU protein, frees GLi1 from SUFU suppression; then, Gli1 is able to enter and be expressed in the nucleus.[37] In this study, we found that hsa_circ_0000069 knockdown could inhibit the expressions of STIL and Gli1 in SW1990 cells in vitro and in SW1990 tumors in vivo. However, when SW1990 cells were treated with hsa_circ_0000069 shRNA2 together with miR-144 antagomir, the effect of hsa_circ_0000069 knockdown on STIL and GLi1 protein expressions were reversed by the miR-144 antagomir. Wu et al found that STIL could promote the proliferation of prostate cancer

cells via regulating MAPK/ERK, PI3K/Akt and AMPK signaling pathways.[40] Collectively, these data indicated that hsa_circ_0000069 knockdown inhibited the growth of pancreatic cancer cells through downregulation of STIL. Those effects could be partially attributed to hsa_circ_0000069 acting as a sponge for miR-144.

Exosomes are potential communicative vectors which are important in the progression of human cancers, including pancreatic cancer.[41,42] Grimolizzi et al reported that exosomes from patients with NSCLC could induce malignant transformation in epithelial cells.[43] Wei et al indicated that gastric cancer cell-derived exosomal miR-15b-3p led to the malignant transformation of gastric mucosa epithelium cells, promoting cell proliferation and migration.[28] In this study, we found that exosomal hsa_circ_0000069 is secreted by SW1990 cells that can be internalized by HPDE cells. In addition, functional experiments demonstrated that SW1990 cell-derived exosomes promoted the proliferation, migration and cell cycle progression of HPDE cells; however, these changes were reversed by exosomes with downregulated hsa_circ_0000069. These data indicated that SW1990 cell-derived exosomes with downregulated hsa_circ_0000069 could inhibit suppress malignant transformation of HPDE cells.

Conclusion

Our results indicated that the expression of hsa_circ_0000069 is significantly upregulated in human pancreatic cancer tissues. Downregulation of hsa_circ_0000069 inhibited proliferation, migration and invasion in pancreatic cancer cells in vitro, and reduced tumor growth in a mouse pancreatic cancer xenograft model. In addition, hsa_circ_0000069 knockdown inhibited the pancreatic cancer progression by sponging miR-1827, thus decreasing the STIL expression. Moreover, SW1990 cell-derived exosomes with downregulated hsa_circ_0000069 could inhibit suppress malignant transformation of HPDE cells. Therefore, targeting the hsa_circ_0000069 might represent a novel therapeutic target for the treatment of pancreatic cancer.

Data Sharing Statement

The data that support the findings of this study are available from the corresponding author upon reasonable request.

Funding

The present study was partially supported by the National Natural Science Foundation of China (no. 81672970), the Natural Science Foundation of Jiangsu Province (no. M2020075), the projects of Suzhou Technology Bureau (nos. SYS201552, SYS2020141 and SYS2018054), found of Suzhou Introduced Team of Clinical Medical Experts (no. SZYJTD201803), Jiangsu Province's Graduate Student Research Innovation Project (no. KYCX19_1986).

Disclosure

Zhenyu Ye and Zhaobi Zhu are co-first authors for this study. The authors declare no competing financial interests.

References

1. Tian J, Zhang R, Piao H, et al. Silencing Tspan1 inhibits migration and invasion, and induces the apoptosis of human pancreatic cancer cells. *Mol Med Rep*. 2018;18:3280–3288.
2. Tuan Anh HL, Tran PT, Thao DT, et al. Degalactotigonin, a steroidal glycoside from solanum nigrum, induces apoptosis and cell cycle arrest via inhibiting the EGFR signaling pathways in pancreatic cancer cells. *Biomed Res Int*. 2018;2018. doi:10.1155/2018/3120972
3. Subramani R, Gonzalez E, Arumugam A, et al. Nimbolide inhibits pancreatic cancer growth and metastasis through ROS-mediated apoptosis and inhibition of epithelial-to-mesenchymal transition. *Sci Rep*. 2016;6:19819. doi:10.1038/srep19819
4. Matsushita Y, Furutani Y, Matsuoka R, Furukawa T. Hot water extract of Agaricus blazei Murrill specifically inhibits growth and induces apoptosis in human pancreatic cancer cells. *BMC Complement Altern Med*. 2018;18:319.
5. Wartenberg M, Cibin S, Zlobec I, et al. Integrated genomic and immunophenotypic classification of pancreatic cancer reveals three distinct subtypes with prognostic/predictive significance. *Clin Cancer Res*. 2018;24:4444–4454. doi:10.1158/1078-0432.CCR-17-3401
6. Andersen DK, Korc M, Petersen GM, et al. Diabetes, pancreatogenic diabetes, and pancreatic cancer. *Diabetes*. 2017;66:1103–1110. doi:10.2337/db16-1477
7. Siegel R, Jemal J, Zou Z, Jemal A. Cancer statistics, 2014. *CA Cancer J Clin*. 2014;64(1):9–29. doi:10.3322/caac.21208
8. Bosetti C, Bertuccio P, Negri E, et al. Pancreatic cancer: overview of descriptive epidemiology. *Mol Carcinog*. 2012;51:3–13. doi:10.1002/mc.20785
9. Jiang LH, Sun DW, Hou JC, Ji ZL. CircRNA: a novel type of biomarker for cancer. *Breast Cancer*. 2018;25:1–7. doi:10.1007/s12282-017-0793-9
10. Chen G, Shi Y, Zhang Y, Sun J. CircRNA_100782 regulates pancreatic carcinoma proliferation through the IL6-STAT3 pathway. *Onco Targets Ther*. 2017;10:5783. doi:10.2147/OTT.S150678
11. Cheng Z, Yu C, Cui S, et al. circTP63 functions as a ceRNA to promote lung squamous cell carcinoma progression by upregulating FOXM1. *Nat Commun*. 2019;10:1–3.
12. Wang K, Long B, Liu F, et al. A circular RNA protects the heart from pathological hypertrophy and heart failure by targeting miR-223. *Eur Heart J*. 2016;37(33):2602–2611. doi:10.1093/eurheartj/ehv713
13. Li H, Hao X, Wang H, et al. Circular RNA expression profile of pancreatic ductal adenocarcinoma revealed by microarray. *Cell Physiol Biochem*. 2016;40:1334–1344. doi:10.1159/000453186
14. Yang J, Cong X, Ren M, et al. Circular RNA hsa_circRNA_0007334 is predicted to promote MMP7 and COL1A1 expression by functioning as a miRNA sponge in pancreatic ductal adenocarcinoma. *J Oncol*. 2019;2019. doi:10.1155/2019/7630894
15. Gao ZQ, Wang JF, Chen DH, et al. Long non-coding RNA GAS5 antagonizes the chemoresistance of pancreatic cancer cells through down-regulation of miR-181c-5p. *Biomed Pharmacother*. 2018;97:809–817. doi:10.1016/j.biopha.2017.10.157

16. Iorio M, Croce CM. MicroRNA dysregulation in cancer: diagnostics, monitoring and therapeutics. A comprehensive review. *EMBO Mol Med*. 2012;4:143–159. doi:10.1002/emmm.201100209
17. Wang H, Tan Z, Hu H, et al. microRNA-21 promotes breast cancer proliferation and metastasis by targeting LZTFL1. *BMC Cancer*. 2019;19:738. doi:10.1186/s12885-019-5951-3
18. Hansen TB, Jensen TI, Clausen BH, et al. Natural RNA circles function as efficient microRNA sponges. *Nature*. 2013;495:384–388. doi:10.1038/nature11993
19. Doyle LM, Wang MZ. Overview of extracellular vesicles, their origin, composition, purpose, and methods for exosome isolation and analysis. *Cells*. 2019;8(7):727. doi:10.3390/cells8070727
20. Liu T, Zhang X, Du L, et al. Exosome-transmitted miR-128-3p increase chemosensitivity of oxaliplatin-resistant colorectal cancer. *Mol Cancer*. 2019;18(1):43.
21. Qu L, Ding J, Chen C, et al. Exosome-transmitted lncARSR promotes sunitinib resistance in renal cancer by acting as a competing endogenous RNA. *Cancer Cell*. 2016;29(5):653–668. doi:10.1016/j.ccell.2016.03.004
22. Li S, Li Y, Chen B, et al. exoRBase: a database of circRNA, lncRNA and mRNA in human blood exosomes. *Nucleic Acids Res*. 2018;46(D1):D106–d112. doi:10.1093/nar/gkx891
23. Zhang X, Wang S, Wang H, et al. Circular RNA circNRIP1 acts as a microRNA-149-5p sponge to promote gastric cancer progression via the AKT1/mTOR pathway. *Mol Cancer*. 2019;18(1):20. doi:10.1186/s12943-018-0935-5
24. Li J, Li Z, Jiang P, et al. Circular RNA IARS (circ-IARS) secreted by pancreatic cancer cells and located within exosomes regulates endothelial monolayer permeability to promote tumor metastasis. *J Exp Clin Cancer Res*. 2018;37(1):177. doi:10.1186/s13046-018-0822-3
25. Zhan Y, Chen Z, Li Y, et al. Long non-coding RNA DANCR promotes malignant phenotypes of bladder cancer cells by modulating the miR-149/MSI2 axis as a ceRNA. *J Exp Clin Cancer Res*. 2018;37(1):273. doi:10.1186/s13046-018-0921-1
26. Au Yeung CL, Co NN, Tsuruga T, et al. Exosomal transfer of stroma-derived miR21 confers paclitaxel resistance in ovarian cancer cells through targeting APAF1. *Nat Commun*. 2016;7:11150. doi:10.1038/ncomms11150
27. Liao J, Liu R, Shi YJ, Yin LH, Pu YP. Exosome-shuttling microRNA-21 promotes cell migration and invasion-targeting PDCD4 in esophageal cancer. *Int J Oncol*. 2016;48(6):2567–2579.
28. Wei S, Peng L, Yang J, et al. Exosomal transfer of miR-15b-3p enhances tumorigenesis and malignant transformation through the DYNLT1/Caspase-3/Caspase-9 signaling pathway in gastric cancer. *J Exp Clin Cancer Res*. 2020;39(1):32.
29. An Y, Cai H, Zhang Y, et al. circZMYM2 competed endogenously with miR-335-5p to regulate JMJD2C in pancreatic cancer. *Cell Physiol Biochem*. 2018;51(5):2224–2236. doi:10.1159/000495868
30. Chen Y, Li Z, Zhang M, et al. Circ-ASH2L promotes tumor progression by sponging miR-34a to regulate Notch1 in pancreatic ductal adenocarcinoma. *J Exp Clin Cancer Res*. 2019;38(1):466. doi:10.1186/s13046-019-1436-0
31. Catalanotto C, Cogoni C, Zardo G. MicroRNA in control of gene expression: an overview of nuclear functions. *Int J Mol Sci*. 2016;17(10):1712. doi:10.3390/ijms17101712
32. Liu Z, Yu Y, Huang Z, et al. CircRNA-5692 inhibits the progression of hepatocellular carcinoma by sponging miR-328-5p to enhance DAB2IP expression. *Cell Death Dis*. 2019;10(12):900.
33. Dong W, Bi J, Liu H, et al. Circular RNA ACVR2A suppresses bladder cancer cells proliferation and metastasis through miR-626/EYA4 axis. *Mol Cancer*. 2019;18(1):95. doi:10.1186/s12943-019-1025-z
34. Aplan PD, Lombardi DP, Kirsch IR. Structural characterization of SIL, a gene frequently disrupted in T-cell acute lymphoblastic leukemia. *Mol Cell Biol*. 1991;11(11):5462–5469. doi:10.1128/MCB.11.11.5462
35. Wang J, Zhang Y, Dou Z, et al. Knockdown of STIL suppresses the progression of gastric cancer by down-regulating the IGF-1/PI3K/AKT pathway. *J Cell Mol Med*. 2019;23(8):5566–5575. doi:10.1111/jcmm.14440
36. Erez A, Castiel A, Trakhtenbrot L, et al. The SIL gene is essential for mitotic entry and survival of cancer cells. *Cancer Res*. 2007;67(9):4022–4027. doi:10.1158/0008-5472.CAN-07-0064
37. Li L, Liu C, Carr AL. STIL: a multi-function protein required for dopaminergic neural proliferation, protection, and regeneration. *Cell Death Discov*. 2019;5:90. doi:10.1038/s41420-019-0172-8
38. Kasai K, Inaguma S, Yoneyama A, Yoshikawa K, Ikeda H. SCL/TAL1 interrupting locus derepresses GLI1 from the negative control of suppressor-of-fused in pancreatic cancer cell. *Cancer Res*. 2008;68(19):7723–7729. doi:10.1158/0008-5472.CAN-07-6661
39. Yu Y, Cheng L, Yan B, et al. Overexpression of Gremlin 1 by sonic hedgehog signaling promotes pancreatic cancer progression. *Int J Oncol*. 2018;53(6):2445–2457.
40. Wu X, Xiao Y, Yan W, Ji Z, Zheng G. The human oncogene SCL/TAL1 interrupting locus (STIL) promotes tumor growth through MAPK/ERK, PI3K/Akt and AMPK pathways in prostate cancer. *Gene*. 2019;686:220–227. doi:10.1016/j.gene.2018.11.048
41. Lan B, Zeng S, Grützmann R, Pilarsky C. The role of exosomes in pancreatic cancer. *Int J Mol Sci*. 2019;20(18):4332. doi:10.3390/ijms20184332
42. Jia Y, Chen Y, Wang Q, et al. Exosome: emerging biomarker in breast cancer. *Oncotarget*. 2017;8(25):41717–41733. doi:10.18632/oncotarget.16684
43. Grimolizzi F, Monaco F, Leoni F, et al. Exosomal miR-126 as a circulating biomarker in non-small-cell lung cancer regulating cancer progression. *Sci Rep*. 2017;7(1):15277. doi:10.1038/s41598-017-15475-6